OXFORD

JNCI J Natl Cancer Inst (2019) 111(11): djz027

doi: 10.1093/jnci/djz027
First published online February 21, 2019
Article

ARTICLE

Differences in Genomic Profiles and Outcomes Between Thoracic and Adrenal Neuroblastoma

Derek A. Oldridge*, Bao Truong*, Douglas Russ, Steven G. DuBois, Zalman Vaksman, Yael P. Mosse, Sharon J. Diskin, John M. Maris†, Katherine K. Matthay†

See the Notes section for the full list of authors' affiliations.
*Authors contributed equally to this work.
†These authors jointly supervised this work.
Correspondence to: Katherine K. Matthay, MD, Department of Pediatrics, UCSF School of Medicine, 550 16th Street, 4th Floor, San Francisco, CA 94158 (e-mail: kate.matthay@ucsf.edu).

Abstract

Background: Neuroblastoma is a biologically and clinically heterogeneous disease. Based on recent studies demonstrating an association between the primary tumor site, prognosis, and commonly measured tumor biological features, we hypothesized that neuroblastomas arising in different sites would show distinct genomic features reflective of the developmental biology of the sympathicoadrenal nervous system.
Methods: We first compared genomic and epigenomic data of primary diagnostic neuroblastomas originating in the adrenal gland (n = 646) compared to thoracic sympathetic ganglia (n = 118). We also evaluated association of common germline variation with these primary sites in 1027 European-American neuroblastoma patients.
Results: We observed higher rates of *MYCN* amplification, chromosome 1q gain, and chromosome 11q deletion among adrenal tumors, which were highly predictive of functional RNA signatures. Surprisingly, thoracic neuroblastomas were more likely to harbor *ALK* driver mutations than adrenal cases among all cases (odds ratio = 1.89, 95% confidence interval = 1.04 to 3.43), and among cases without *MYCN* amplification (odds ratio = 2.86, 95% confidence interval = 1.48 to 5.49). Common germline single nucleotide polymorphisms (SNPs) in *BARD1* (previously associated with high-risk neuroblastoma) were found to be strongly associated with predisposition for origin at adrenal, rather than thoracic, sites.
Conclusions: Neuroblastomas arising in the adrenal gland are more likely to harbor structural DNA aberrations including *MYCN* amplification, whereas thoracic tumors show defects in mitotic checkpoints resulting in hyperdiploidy. Despite the general association of *ALK* mutations with high-risk disease, thoracic tumors are more likely to harbor gain-of-function *ALK* aberrations. Site of origin is likely reflective of stage of sympathetic nervous system development when malignant transformation occurs and is a surrogate for underlying tumor biology.

Neuroblastoma is an embryonal malignancy of the sympathetic nervous system that remains responsible for 10% of all childhood cancer deaths (1,2). It is a highly heterogeneous disease, with diverse clinical presentations, biologic features, and outcomes, creating both challenges and opportunities in risk stratification and identification of therapeutic targets. Studies over several decades have revealed several important recurrent genetic alterations including *MYCN* amplification, large-scale chromosomal aberrations, and gain-of-function *ALK* mutations (3). A recent study established a relationship between the primary tumor site, prognosis, and some tumor biological features (4). A key finding was that *MYCN* amplification was statistically significantly more common among adrenal tumors compared with nonadrenal tumors and statistically significantly less common among thoracic compared with nonthoracic tumors. To refine and extend these findings, here we compared genomic features between neuroblastomas arising from adrenal and thoracic primary tumor sites using the Therapeutically Applicable

Received: September 16, 2019; **Revised:** January 10, 2019; **Accepted:** February 7, 2019
© The Author(s) 2019. Published by Oxford University Press. All rights reserved. For permissions, please email: journals.permissions@oup.com

Research to Generate Effective Treatments (TARGET) and genome-wide association study (GWAS) datasets.

Methods

Data Sources

Two different datasets were utilized for this study. First, we compared the genomic changes in adrenal vs thoracic tumors using genome-scale data from primary neuroblastoma cases included in the TARGET project (https://ocg.cancer.gov/programs/target/data-matrix). Because not all genomic data modalities were available for each individual TARGET case, we conducted separate genomic analyses for each subcohort in which the data were available (Supplementary Figure 1 and Supplementary Table 1, available online). Second, we assessed association of common germline variation with primary site in an overlapping cohort of European-American neuroblastoma patients. Informed consent for the Children's Oncology Group (COG) Neuroblastoma Biology Study was obtained at each COG institution where respective patients were treated. Tumor samples without identifiers were sent to the Children's Hospital of Philadelphia, and therefore these studies were exempt from human subject research guidelines, as confirmed by the institutional review boards at Children's Hospital of Philadelphia (CHOP) and University of California San Francisco (UCSF). Tumors were classified as "adrenal" (n = 646) or "thoracic" (n = 118) when Systematized Nomenclature of Medicine (SNOMED) annotation was sufficiently detailed to make a definitive call of primary site.

Statistical Methods for Clinical Association Testing

All statistical calculations, association testing, and data visualization were performed in the R programming language. Binary variable associations with adrenal vs thoracic tumors (including discrete clinical covariates and DNA mutations) were evaluated by two-sided Fisher-exact test, and 95% confidence intervals were computed using the CRAN respository package "exact2x2" with default parameters. Unless otherwise specifed, all tests were two-sided and *P* values less than .05 were considered statistically significant. Survival analyses including Kaplan-Meier plot visualization, log-rank association testing, and multivariable Cox proportional hazard modeling were performed using the CRAN respository package "survival." Event-free survival (EFS) was defined as time from diagnosis to first episode of death, second malignancy, or progression/relapse, with patients without event censored at time of last follow-up. Separate analyses were performed for all adrenal and thoracic samples and for only *MYCN*-nonamplified adrenal and thoracic samples. Cox proportional hazard modeling was used to assess association of primary site with survival, adjusting for *MYCN* amplification, age at least 18 months, and stage 4 vs other stage disease. To address violation of the proportional hazard assumption identified by examination of Schoenfeld residuals, we incorporated covariate-survival time interaction terms into the model as previously described, using a split-time of 1 year (https://socialsciences.mcmaster.ca/jfox/Books/Companion/appendices/Appendix-Cox-Regression.pdf).

Computational and Statistical Methods for Genomic Data Analysis

Unless otherwise specified, processed genomic datasets from the TARGET project were downloaded and utilized as-is (https://ocg.cancer.gov/programs/target/data-matrix). For GWAS analysis, statistical tests of association for common germline single nucleotide polymorphisms (SNPs) were performed using SNPTEST software with an additive genetic model. SNP alleles are reported with respect to the positive strand of the hg19 human reference genome except for rs6720708, rs17489363, and rs2168101; these are reported on the negative strand for consistency with BARD1 and LMO1 literature. Detailed computational methods for processing, normalization, and statistical analysis for the referenced genomic datasets—including SNP, gene expression, and DNA methylation microarrays; whole genome sequencing (WGS); whole exome sequencing (WES); and targeted gene panel sequencing data—are included in Supplementary Methods (available online).

Results

Clinical Associations With Neuroblastoma Site of Origin

Within the TARGET neuroblastoma cohort (n = 1180), primary tumors that arose from the adrenal gland (n = 646) were associated with inferior patient outcomes in comparison with primary thoracic tumors (n = 118), including reduced EFS ($P = .006$) and overall (OS; $P < .001$) survival (Figure 1, A and B). Missing or ambiguous primary site annotation (n = 373) or small cohort numbers (eg, n = 22 head/neck and n = 21 and pelvic cases) precluded meaningful analysis of the remaining cases. Primary adrenal tumors associated with a number of negative prognostic factors including age at least 18 months (odds ratio [OR] = 2.83, 95% confidence interval [CI] = 1.89 to 4.24, $P < .001$), International Neuroblastoma Staging System (5) (INSS) stage 4 disease (OR = 3.06, 95% CI = 2.03 to 4.61, $P < .001$), COG high-risk disease (OR = 4.78, 95% CI = 3.16 to 7.34, $P < .001$) (6), and *MYCN* amplification (OR = 8.57, 95% CI = 3.74 to 20.37, $P < .001$) compared with their thoracic counterparts within the TARGET cohort (Table 1). Whereas 31.5% (201 of 638) of primary adrenal tumors were *MYCN*-amplified, only 5.1% (6 of 118) of primary thoracic tumors were *MYCN*-amplified. Restricting our analysis to the remaining *MYCN*-nonamplified cases, we observed persistent associations of adrenal compared with thoracic cases with reduced EFS ($P = .04$) and OS ($P < .001$; Figure 1, C and D), age at least 18 months (OR = 2.55, 95% CI = 1.66 to 3.91, $P < .001$), as well as increased likelihood of INSS stage 4 (OR = 2.35, 95% CI = 1.53 to 3.60, $P < .001$) and high-risk (OR = 3.22, 95% CI = 2.07 to 5.04, $P < .001$) disease.

These inferior patient outcomes were then validated in the CHOP GWAS neuroblastoma cohort (n = 6407) when comparing adrenal (n = 2501) to thoracic (n = 906) primary tumors, including both reduced EFS ($P < .001$) and OS ($P < .001$) (Figure 1, E and F). Primary adrenal tumors were again more likely to have *MYCN* amplification (OR = 9.08, 95% CI = 6.17 to 13.41, $P < .001$), INSS Stage 4 disease (OR = 4.93, 95% CI = 4.10 to 5.94, $P < .001$), COG high-risk disease (OR = 6.21, 95% CI = 5.06 to 7.64, $P < .001$), and age at least 18 months (OR = 1.38, 95% CI = 1.18 to 1.61, $P < .001$). Considering only *MYCN*-nonamplified tumors, adrenal disease was still associated with inferior EFS ($P < .001$) and OS ($P < .001$) (Figure 1, G and H), and a higher likelihood of INSS Stage 4 (OR = 3.63, 95% CI = 2.95 to 4.46, $P < .001$) and high-risk (OR = 4.01, 95% CI = 3.16 to 5.10, $P < .001$) disease; however, an association with age at least 18 months was no longer observed (OR = 1.14, 95% CI = 0.97 to 1.35, $P = .13$). These findings suggest that differences in the frequency of *MYCN* amplification cannot completely account for inferior clinical outcomes observed in

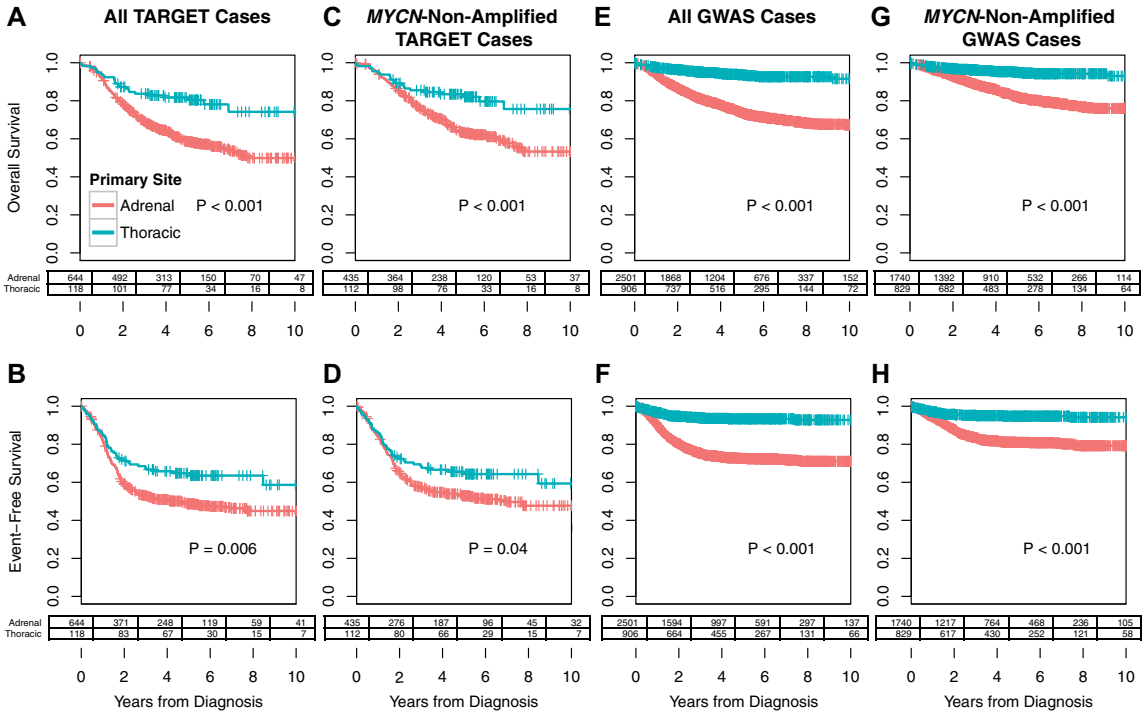

Figure 1. Survival analysis comparing adrenal vs thoracic primary site. Comparison of (**A**) overall survival (OS) and (**B**) event-free survival (EFS) for 646 adrenal tumors and 118 thoracic tumors in the Therapeutically Applicable Research to Generate Effective Treatments (TARGET) cohort. **C**) OS and (**D**) EFS for 437 adrenal tumors and 112 thoracic tumors in the TARGET cohort that are *MYCN*-nonamplified. **E**) OS and (**F**) EFS for 2501 adrenal tumors and 906 thoracic tumors in the = Children's Hospital of Philadelphia (CHOP) genome-wide association study (GWAS) cohort. **G**) OS and (**H**) EFS for 1740 adrenal tumors and 829 thoracic tumors in the CHOP GWAS cohort that are *MYCN*-nonamplified. *P* values are computed by two-sided log-rank test. Cross marks illustrate censored data points. Remaining patient counts at specified incremental 2-year cutoffs are shown in the table below each survival curve. The superior EFS and OS in the GWAS cases can be explained by the fact that the TARGET analysis included a higher proportion of tumors in the high-risk category (Table 1).

neuroblastomas arising in the adrenal gland compared with the thorax.

By multivariable Cox-proportional hazard modeling, adrenal neuroblastoma was an independent predictor of worse OS in the GWAS cohort ($P < .001$), but not in the comparatively smaller TARGET cohort ($P = .28$), after adjusting for *MYCN* amplification status, disease stage, and age of at least 18 months. Adrenal neuroblastoma was not an independent predictor of worse EFS by similar multivariable analysis for either the GWAS ($P = .09$) or TARGET ($P = .67$) cohorts.

Copy Number Alterations and Their Association With Neuroblastoma Site of Origin

To perform an unbiased assessment of somatic copy number alterations that differ between primary adrenal vs thoracic neuroblastomas, we analyzed tumor/normal data from SNP microarray or from several different Next Generation Sequencing platforms available through the TARGET project at 1-Mb resolution. Consistent with the observed association based on clinical data alone, we observed higher rates of *MYCN* amplification in adrenal vs thoracic neuroblastomas by WGS, WES, targeted panel sequencing, and SNP microarrays separately and by cross-platform meta-analysis (Figure 2A). Besides *MYCN*, no other focal copy number alterations were differentially enriched between adrenal and thoracic neuroblastomas after multiple test correction.

Because large segmental copy number alterations are highly prevalent and prognostically relevant in neuroblastoma (7), we repeated our differential copy number analysis focusing specifically on chromosomal arms. We observed enrichment of chromosome 1p loss and 1q gain in adrenal compared with thoracic neuroblastomas, whereas loss of chromosomes 3q, 4q, 16 (p&q), 19 (p&q), and X (p&q) as well as gain of 17p were all enriched in thoracic relative to adrenal neuroblastomas (false discovery rate [FDR] < 0.05; Figure 2B). Because chromosome 1p loss and 1q gain are highly correlated with *MYCN* amplification, whereas 11q loss is highly anticorrelated (8,9), we further restricted our analysis to only *MYCN*-nonamplified cases to remove confounding by MYCN status. Whereas associations of chromosome 1q gain with adrenal and chromosome 19q loss with thoracic neuroblastomas persisted (FDR < 0.05) in the subset of *MYCN*-nonamplified patients, we observed enrichment of chromosome 11q loss in adrenal relative to thoracic neuroblastomas that was not evident when considering all patients regardless of *MYCN* status (Figure 2, A and B).

Point Mutations and Their Association With Neuroblastoma Site of Origin

Activating point mutations in the *ALK* oncogene have emerged as promising targets for rational therapy in neuroblastoma (10–13). We observed that 52 of 559 adrenal cases (9.3%) harbored *ALK* mutations compared with 18 of 111 thoracic cases (16.2%), reflecting a statistically significant enrichment of *ALK* mutations in thoracic compared with adrenal neuroblastomas (OR = 1.89, 95% CI = 1.04 to 3.43, $P = .04$; Figure 3). Moreover, in the subset of *MYCN*-nonamplified neuroblastoma, we observed

ARTICLE

Table 1. Clinical and biological features in adrenal vs thoracic neuroblastoma

Clinical subgroups	Adrenal neuroblastomaNo. (%)	Thoracic neuroblastomaNo. (%)	OR (95% CI)
All adrenal and thoracic cases included in TARGET cohort			
Age			
≥ 18 months	486 (75.2)	61 (51.7)	2.83 (1.89 to 4.24)
<18 months	160 (24.8)	57 (48.3)	1.00 (Ref)
Stage			
4	499 (77.2)	62 (52.5)	3.06 (2.03 to 4.61)
Not 4	147 (22.8)	56 (47.5)	1.00 (Ref)
COG risk profile			
High risk	507 (78.5)	51 (43.2)	4.78 (3.16 to 7.34)
Not high risk	139 (21.5)	67 (56.8)	1.00 (Ref)
MYCN status			
MYCN-amplified	201 (31.5)	6 (5.1)	8.57 (3.74 to 20.37)
MYCN-nonamplified	437 (68.5)	112 (94.9)	1.00 (Ref)
Only TARGET cases without MYCN amplification			
Age			
≥ 18 months	314 (71.9)	56 (50.0)	2.55 (1.66 to 3.91)
<18 months	123 (28.1)	56 (50.0)	1.00 (Ref)
Stage			
4	310 (70.9)	57 (50.9)	2.35 (1.53 to 3.60)
Not 4	127 (29.1)	55 (49.1)	1.00 (Ref)
COG risk profile			
High risk	299 (68.4)	45 (40.2)	3.22 (2.07 to 5.04)
Not high risk	138 (31.6)	67 (59.8)	1.00 (Ref)
All adrenal and thoracic cases included in CHOP GWAS cohort			
Age			
≥ 18 months	1419 (56.7)	442 (48.8)	1.38 (1.18 to 1.61)
<18 months	1082 (43.3)	464 (51.2)	1.00 (Ref)
Stage			
4	1349 (54.0)	174 (19.2)	4.93 (4.10 to 5.94)
Not 4	1150 (46.0)	731 (80.8)	1.00 (Ref)
COG risk profile			
High risk	1279 (52.5)	132 (15.1)	6.21 (5.06 to 7.64)
Not high risk*	1157 (47.5)	742 (84.9)	1.00 (Ref)
MYCN status			
MYCN-amplified	553 (24.1)	29 (3.4)	9.08 (6.17 to 13.41)
MYCN-nonamplified	1740 (75.9)	829 (96.6)	1.00 (Ref)
Chromosome 11q status†			
11q LOH	242 (19.8)	54 (10.5)	2.09 (1.52 to 2.90)
No 11q LOH	983 (80.2)	459 (89.5)	1.00 (Ref)
Only CHOP GWAS cases without MYCN amplification			
Age			
≥18 months	878 (50.5)	391 (47.2)	1.14 (0.97 to 1.35)
<18 months	862 (49.5)	438 (52.8)	1.00 (Ref)
Stage			
4	743 (42.7)	141 (17.0)	3.63 (2.95 to 4.46)
Not 4	996 (57.3)	687 (83.0)	1.00 (Ref)
COG risk profile			
High risk	592 (34.6)	95 (11.6)	4.01 (3.16 to 5.10)
Not high risk*	1121 (65.4)	721 (88.4)	1.00 (Ref)
Chromosome 11q status†			
11q LOH	220 (22.9)	52 (10.6)	2.52 (1.81 to 3.50)
No 11q LOH	739 (77.1)	440 (89.4)	1.00 (Ref)

*Ref refers to the reference group for the OR, which is the clinical subgroup associated with favorable prognosis and is enriched in thoracic cases and anticorrelated with adrenal cases. CI = confidence interval; CHOP = Children's Hospital of Philadelphia; COG = Children's Oncology Group; GWAS = genome-wide association study; LOH = loss of heterozygosity; OR = odds ratio; TARGET = Therapeutically Applicable Research to Generate Effective Treatments.

†Clinical annotation of tumor chromosome 11q status is available only for the GWAS cohort, not for the TARGET cohort; association of 11q loss with primary site in the TARGET cohort was therefore performed by bioinformatic copy number analysis using available genomic data (Figure 2).

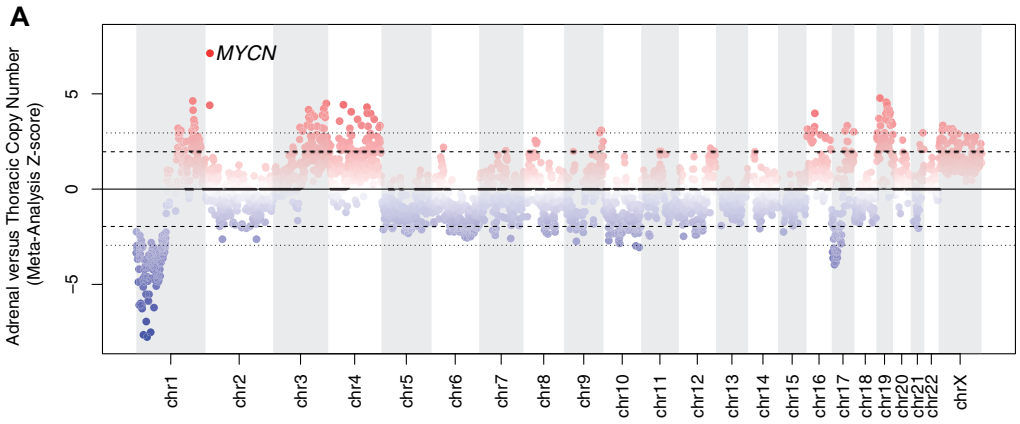

B

All Cases

	Avg Adrenal	Avg Thoracic	Avg Difference	Meta Z-score	Meta P-value	Meta FDR
1p	−0.09	+0.00	−0.10	**−7.072**	**< 0.001**	**< 0.001**
1q	+0.07	+0.04	+0.03	**+2.749**	**0.006**	**0.022**
2p	+0.11	+0.11	+0.00	+0.331	0.740	0.829
2q	+0.05	+0.08	−0.03	−1.982	0.047	0.147
3p	−0.13	−0.15	+0.01	+0.801	0.423	0.694
3q	−0.04	−0.09	+0.05	**+3.513**	**< 0.001**	**0.003**
4p	−0.07	−0.10	+0.03	+1.877	0.060	0.165
4q	−0.03	−0.08	+0.05	**+3.498**	**< 0.001**	**0.003**
5p	−0.00	+0.02	−0.02	−1.553	0.120	0.274
5q	+0.00	+0.03	−0.03	−2.023	0.043	0.147
6p	+0.04	+0.03	+0.01	+0.430	0.667	0.807
6q	+0.03	+0.05	−0.02	−1.285	0.199	0.388
7p	+0.13	+0.15	−0.02	−1.561	0.119	0.274
7q	+0.16	+0.17	−0.01	−0.742	0.458	0.722
8p	+0.01	−0.01	+0.02	+1.299	0.194	0.388
8q	−0.01	−0.02	+0.01	+0.441	0.659	0.807
9p	−0.08	−0.08	+0.00	+0.005	0.996	0.996
9q	−0.04	−0.07	+0.03	+1.958	0.050	0.147
10p	−0.07	−0.05	−0.01	−1.203	0.229	0.427
10q	−0.08	−0.06	−0.02	−1.740	0.082	0.210
11p	−0.01	−0.02	+0.01	+0.401	0.688	0.807
11q	−0.16	−0.16	−0.01	−0.299	0.765	0.829
12p	+0.06	+0.07	−0.01	−1.025	0.305	0.522
12q	+0.08	+0.09	−0.00	−0.401	0.689	0.807
13q	+0.06	+0.07	−0.01	−0.557	0.578	0.789
14q	−0.09	−0.10	+0.01	+0.596	0.551	0.779
15q	−0.04	−0.03	−0.01	−0.666	0.506	0.768
16p	−0.04	−0.08	+0.04	**+2.803**	**0.005**	**0.021**
16q	−0.02	−0.07	+0.05	**+3.208**	**0.001**	**0.008**
17p	+0.05	+0.12	−0.07	**−3.724**	**< 0.001**	**0.002**
17q	+0.28	+0.28	+0.00	+0.064	0.949	0.973
18p	+0.05	+0.07	−0.02	−1.064	0.287	0.512
18q	+0.09	+0.09	−0.00	−0.295	0.768	0.829
19p	−0.08	−0.15	+0.07	**+3.773**	**< 0.001**	**0.002**
19q	−0.06	−0.13	+0.06	**+4.190**	**< 0.001**	**0.001**
20p	+0.02	+0.02	+0.01	+0.446	0.655	0.807
20q	+0.03	+0.02	+0.01	+0.633	0.527	0.772
21q	−0.04	−0.06	+0.02	+1.293	0.196	0.388
22q	+0.02	+0.02	+0.00	+0.176	0.860	0.905
Xp	−0.16	−0.24	+0.08	**+3.059**	**0.002**	**0.011**
Xq	−0.16	−0.24	+0.07	**+2.849**	**0.004**	**0.020**

MYCN-Non-Amplified Cases

	Avg Adrenal	Avg Thoracic	Avg Difference	Meta Z-score	Meta P-value	Meta FDR
1p	−0.02	+0.01	−0.03	−2.646	0.008	0.061
1q	+0.07	+0.04	+0.03	**+2.921**	**0.003**	**0.048**
2p	+0.09	+0.10	−0.01	−0.722	0.470	0.704
2q	+0.04	+0.07	−0.03	−2.043	0.041	0.180
3p	−0.17	−0.14	−0.03	−1.622	0.105	0.307
3q	−0.04	−0.08	+0.04	+2.759	0.006	0.059
4p	−0.12	−0.11	−0.01	−0.705	0.481	0.704
4q	−0.06	−0.08	+0.02	+1.404	0.160	0.346
5p	−0.01	+0.02	−0.03	−1.682	0.093	0.292
5q	−0.00	+0.03	−0.03	−2.436	0.015	0.076
6p	+0.05	+0.03	+0.03	+1.966	0.049	0.184
6q	+0.04	+0.05	−0.00	−0.305	0.761	0.914
7p	+0.16	+0.15	+0.00	+0.101	0.920	0.943
7q	+0.20	+0.17	+0.02	+1.505	0.132	0.318
8p	+0.01	−0.00	+0.01	+0.567	0.571	0.772
8q	−0.02	−0.02	−0.00	−0.040	0.968	0.968
9p	−0.08	−0.08	−0.00	−0.266	0.790	0.914
9q	−0.05	−0.07	+0.01	+0.925	0.355	0.560
10p	−0.07	−0.05	−0.02	−1.794	0.073	0.249
10q	−0.08	−0.06	−0.02	−1.478	0.140	0.318
11p	−0.01	−0.00	−0.00	−0.224	0.823	0.914
11q	−0.22	−0.16	−0.06	**−2.972**	**0.003**	**0.048**
12p	+0.07	+0.07	−0.00	−0.193	0.847	0.914
12q	+0.10	+0.09	+0.01	+0.981	0.327	0.548
13q	+0.08	+0.07	+0.01	+0.554	0.579	0.772
14q	−0.11	−0.10	−0.02	−0.985	0.325	0.548
15q	−0.04	−0.03	−0.01	−0.966	0.334	0.548
16p	−0.06	−0.08	+0.03	+2.015	0.044	0.180
16q	−0.03	−0.07	+0.04	+2.614	0.009	0.061
17p	+0.09	+0.12	−0.03	−1.586	0.113	0.308
17q	+0.31	+0.28	+0.03	+1.496	0.135	0.318
18p	+0.06	+0.07	−0.01	−0.501	0.617	0.790
18q	+0.10	+0.09	+0.01	+0.548	0.584	0.772
19p	−0.11	−0.15	+0.05	+2.543	0.011	0.064
19q	−0.08	−0.12	+0.05	**+3.027**	**0.002**	**0.048**
20p	+0.02	+0.01	+0.00	+0.348	0.728	0.904
20q	+0.03	+0.03	+0.00	+0.196	0.845	0.914
21q	−0.06	−0.05	−0.01	−0.987	0.324	0.548
22q	+0.02	+0.02	+0.00	+0.159	0.873	0.918
Xp	−0.20	−0.24	+0.04	+1.291	0.197	0.403
Xq	−0.20	−0.24	+0.03	+1.188	0.235	0.459

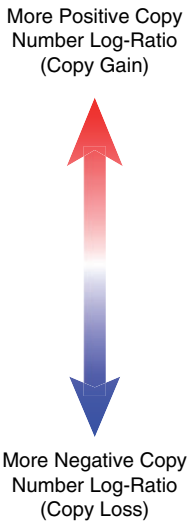

Figure 2. Adrenal vs thoracic tumor copy number association analysis. **A**) Meta-analysis by nonoverlapping 1-Mb tiles. The y-axis reflects an inverse variance-weighted meta-analysis across four datasets—single nucleotide polymorphism (SNP) microarray, whole genome sequencing, whole exome sequencing, and gene panel sequencing cohorts—of average log-ratio (tumor normalized to normal) differences between adrenal vs thoracic cases divided by SD (z score). A positive z score (**red**) implies that the relative copy number is higher in adrenal vs thoracic cases and a negative z score (**blue**) implies the opposite. The **inner dashed line** illustrates the z score corresponding to a nominal *P* value cut point of .05, and the **outer dotted line** illustrates the z score corresponding to a multiple test-adjusted false discovery rate (FDR) cut point of 0.05. The 1-Mb bin containing *MYCN* is labeled, because it is the only focal copy number alteration to reach statistical significance. **B**) Meta-analysis by chromosome arm. "Avg Adrenal" and "Avg Thoracic" denote a weighted average copy number log-ratio for adrenal and thoracic cases, respectively. More positive/**red** values reflect regions of greater copy number gain and more negative/**blue** values reflect regions of greater copy number loss. From the difference of these values (Avg Difference), a z score and two-tailed *P* value were computed by inverse-variance meta-analysis. The FDR was controlled by the Benjamini-Hochberg method. Results with multiple test-adjusted statistical significance at FDR less than 0.05 are **bolded.**

ARTICLE

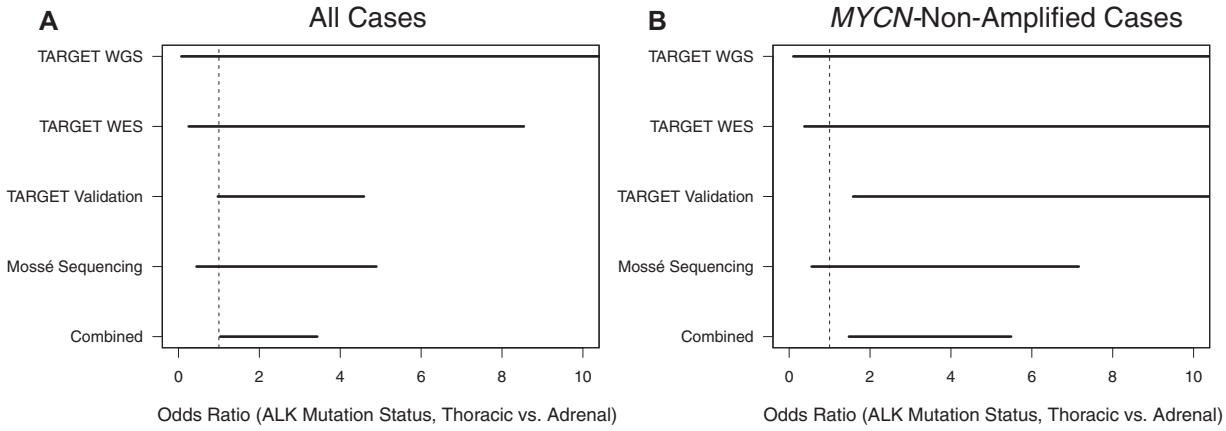

Figure 3. Association of ALK-driver mutations with primary site. **A)** Association results of all available Therapeutically Applicable Research to Generate Effective Treatments (TARGET) adrenal and thoracic cases across four sequencing subcohorts/platforms. The measured odds ratio for each analysis is shown as a **black dot** and the corresponding 95% confidence interval is shown as a **solid line**. In the combined analysis of n = 559 unique adrenal and n = 111 unique thoracic patients, there was a statistically significant enrichment of ALK mutations in thoracic relative to adrenal cases (odds ratio = 1.89, 95% confidence interval = 1.04 to 3.43, Fisher exact $P = .04$). **B)** Similar to the analysis in **(A)** except restricting only to the *MYCN*-nonamplified subset (n = 372 unique adrenal and n = 105 unique thoracic cases). The enrichment of ALK mutations in thoracic neuroblastoma is even more pronounced in the *MYCN*-nonamplified subset (odds ratio = 2.86, 95% confidence interval = 1.48 to 5.49, Fisher exact $P = .003$). WES = whole exome sequencing; WGS = whole genome sequencing.

that 25 of 372 adrenal cases (6.7%) harbored *ALK* mutations compared with 18 of 105 thoracic cases (17.1%), demonstrating an even stronger enrichment of *ALK* mutations in thoracic compared with adrenal neuroblastoma in the absence of *MYCN* amplification (OR = 2.86, 95% CI = 1.48 to 5.49, $P = .003$; Figure 3). Furthermore, after adjusting for high-risk disease in a logistic regression model of *ALK* mutation status in *MYCN*-nonamplified neuroblastoma, the association of primary site with *ALK* mutation status persisted ($P = .02$; Supplementary Figure 2, available online). Taken together, these results suggest that the increased prevalence of *ALK* mutations observed in thoracic neuroblastoma is independent of *MYCN* amplification status or high-risk disease.

We did not observe statistically significant differences in the type of *ALK* mutations (eg, F1174L vs R1275Q) that occurred in adrenal and thoracic neuroblastomas (Supplementary Figure 3, available online). Aside from *ALK*, we did not observe statistically significant differences in mutation frequencies for other individual genes, although our statistical power is limited by the low rate of recurrent somatic mutations in neuroblastoma. There was no statistically significant difference in the overall somatic coding mutation frequency between adrenal (median = 17 WES mutations, 13 WGS mutations) vs thoracic (median = 17 WES mutations, 14.5 WGS mutations) cases (WGS Wilcoxon $P = .59$, WES Wilcoxon $P = .74$).

Functional Genomic Associations With Neuroblastoma Site of Origin

To evaluate the relationship of primary site with functional subclasses of neuroblastoma, we performed unsupervised hierarchical clustering on adrenal (n = 143) and thoracic (n = 19) cases with RNA expression profiling obtained by HuEx microarray, as well as adrenal (n = 128) and thoracic (N = 15) cases with DNA methylation profiling by Infinium microarray. The strongest clustering was observed for *MYCN*-amplified cases regardless of primary site, suggesting that known genetic lesions are the principal drivers of functional genomic signatures in neuroblastoma (Figure 4A). Additionally, global DNA methylation patterns show strong clustering by *MYCN* amplification status with weaker clustering by tumor primary site (Figure 4B). We observed similarly weak clustering by primary tumor location when restricting to *MYCN*-nonamplified cases (Supplementary Figure 4A-B, available online).

Complementary to the copy number results, we observed strong differential activation of *MYCN* signaling expression signatures in adrenal relative to thoracic cases by Gene Set Enrichment Analysis (Supplementary Figure 5, available online). Moreover, the degree to which chromosome arm-based positional gene sets were differentially expressed between adrenal and thoracic neuroblastomas was highly correlated with the observed differences in DNA copy number (Spearman's rho = 0.82, $P < .001$; Supplementary Figure 6A, available online) and persisted when restricting to *MYCN*-nonamplified disease (Spearman's rho = 0.61, $P < .001$; Supplementary Figure 6B, available online).

Due to the prominence of genetic lesions for predicting neuroblastoma expression signatures, we performed a *limma* (Linear Models for Microarray Data) differential gene expression analysis between adrenal and thoracic neuroblastomas adjusting for MYCN amplification and chromosome 11q loss, which are mutually exclusive and each highly associated with poor outcome. Whereas we observed 3892 differentially expressed genes based on MYCN amplification status and 226 differentially expressed genes based on chromosome 11q copy number status, there were no differentially expressed genes associated with adrenal vs thoracic neuroblastoma after adjusting for MYCN amplification and chromosome 11q loss (statistical significance defined by FDR < 0.01, 22 985 total genes tested), underscoring that RNA expression differences observed between adrenal and thoracic neuroblastomas are largely predicted by underlying genetic lesions. We do observe higher RNA expression of *MYC* in *MYCN*-nonamplified cases ($P < .001$; Supplementary Figure 7, available online), suggesting that MYC overexpression may be a contributing factor in *MYCN*-nonamplified disease.

Correlation of Common Germline Variants With Neuroblastoma Site of Origin

We conducted an unbiased GWAS of our European-American discovery cohort (707 adrenal cases vs 320 ancestry-matched

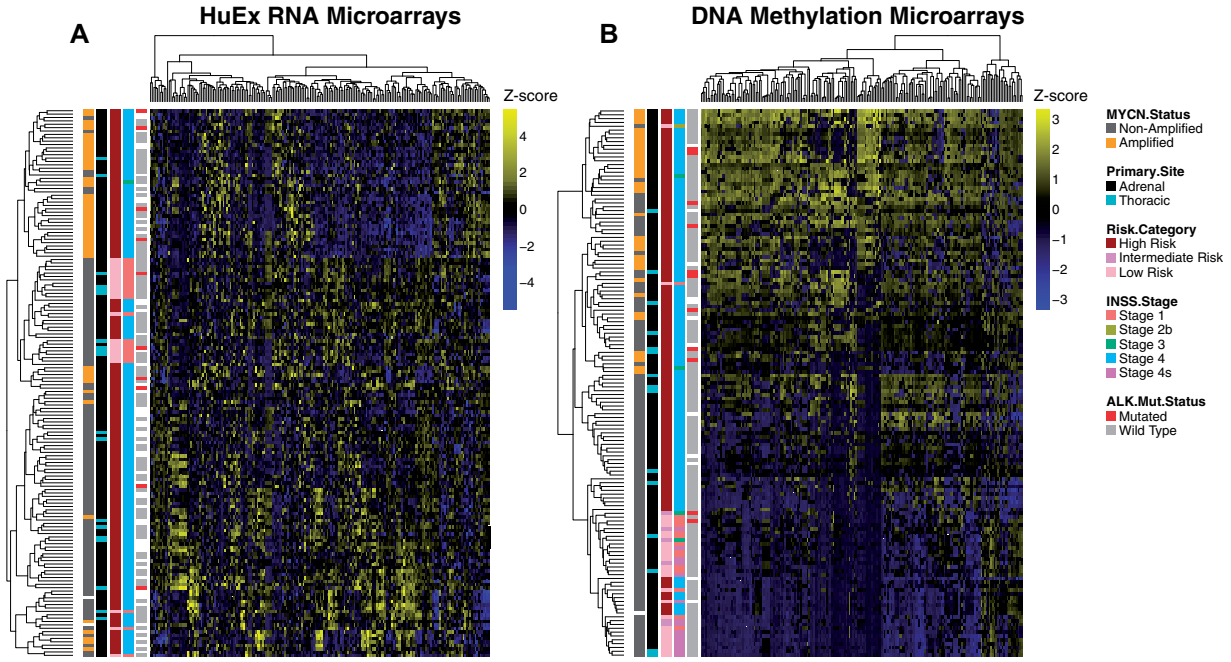

Figure 4. Unbiased clustering analysis of functional genomic and DNA methylation data in the Therapeutically Applicable Research to Generate Effective Treatments (TARGET) cohort. Heatmaps and hierarchical clustering for all adrenal and thoracic (**A**) HuEx RNA microarray samples and (**B**) DNA methylation microarray samples. Rows reflect independent patient profiles and columns reflect the 200 probesets with the highest variance after (**A**) log2 transformation of RNA probe intensity and (**B**) logit transformation of methylation beta values. Columns are mean-centered and normalized by SD (z score transformation) and illustrated on a **blue-yellow scale**. Additional **colored boxes** illustrate clinical annotations for each patient according to the legend (**white** = missing annotation).

thoracic cases, inflation factor = 1.01), and observed the strongest association signal with adrenal primary compared with thoracic at the *BARD1* gene locus (see Figure 5). The most highly associated SNP, rs6720708 (alleles = T/C, adrenal-associated allele = T; OR = 1.74, 95% CI = 1.44 to 2.12, $P = 1.99 \times 10^{-8}$), falls within the locus identified by our original *BARD1* GWAS study (14) and exhibits strong linkage disequilibrium with the rs17489363 SNP ($R^2 = 0.908$, D' = 0.989). The T-allele of rs17489363 was recently proposed to increase high-risk neuroblastoma susceptibility by disrupting HSF1 transcription factor binding at the *BARD1* promoter, thereby reducing expression of the BARD1 tumor suppressor (15). This rs17489363 association is recapitulated between adrenal and thoracic neuroblastomas (alleles = T/C, adrenal-associated allele = T; OR = 1.64, 95% CI = 1.36 to 1.98, $P = 3.10 \times 10^{-7}$), persists in MYCN-nonamplified cases (adrenal-associated allele = T; OR = 1.65, 95% CI = 1.33 to 2.04, $P = 4.49 \times 10^{-6}$), and replicates in an independent European-American cohort (484 adrenal cases vs 242 thoracic cases) genotyped on the Omni array platform (adrenal-associated allele = T; OR = 1.39, 95% CI = 1.11 to 1.73, $P = .003$).

We also observed that an SNP within *CASC15* that was previously associated with high-risk neuroblastoma nominally associated with adrenal primary site (rs6939340, alleles = A/G, adrenal-associated allele = G, OR = 1.30, 95% CI = 1.08 to 1.57, $P = .005$) and replicated in the independent Omni array cohort (adrenal-associated allele = G; OR = 1.37, 95% CI = 1.10 to 1.70, $P = .005$). There was no statistically significant differential association between adrenal and thoracic neuroblastomas for other SNPs that have been previously associated with neuroblastoma at the *HACE1* (rs4336470, alleles = C/T, adrenal-favored allele = C, OR = 1.14, 95% CI = 0.92 to 1.39, $P = .23$), *LIN28B* (rs17065417, alleles = A/C, adrenal-favored allele = A, OR = 1.32, 95% CI = 0.91 to 1.90, $P = .14$), or *LMO1* (rs2168101, alleles = G/T, adrenal-favored allele = G, OR = 1.14, 95% CI = 0.88 to 1.46, $P = .32$) loci.

Discussion

Our study validates and extends our prior finding that *MYCN* amplification is less common and survival is improved in thoracic compared with adrenal neuroblastoma. The biological mechanism by which *MYCN* amplification leads to aggressive high-risk disease is unclear, although prior evidence points to expansive roles of MYCN in multiple aspects of tumorigenesis and metastasis, including immune regulation, cell adhesion, cell proliferation, and angiogenesis (16). It is therefore not surprising that the higher rate of *MYCN* amplification among adrenal neuroblastoma correlates with poor outcomes. *MYCN*-nonamplified adrenal neuroblastoma were more likely to have high-risk disease and had poorer EFS and OS rates compared with *MYCN*-nonamplified thoracic cases in our study. Together with findings from prior studies (4), our results support the hypothesis that *MYCN* amplification does not fully explain poorer outcomes seen in adrenal neuroblastoma. A subset of *MYCN*-nonamplified neuroblastoma may nonetheless express high levels of MYC protein, contributing to inferior outcomes in this setting (17). Although we did not measure MYC protein expression directly, our observation of higher *MYC* RNA expression in *MYCN*-nonamplified cases suggests that MYC overexpression may be a contributing factor.

Our study therefore investigated other potential genomic features to differentiate adrenal and thoracic neuroblastoma. Many statistically significant differences in segmental chromosomal alterations between adrenal and thoracic cohorts (prevalence of 1p loss in adrenal neuroblastoma and losses of 3q, 4q, 16p/q, and 19p/q as well as gain of 17p in thoracic

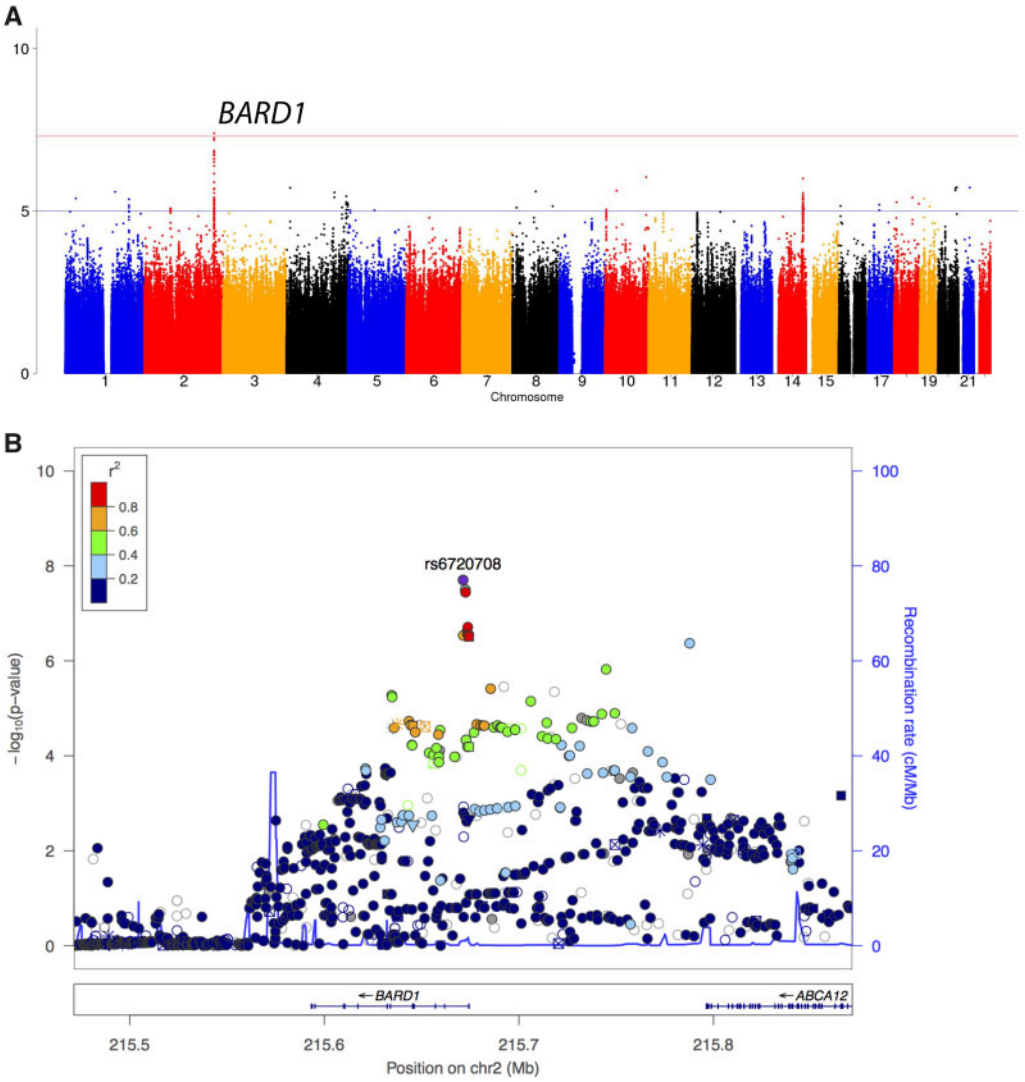

Figure 5. Genome-wide association study results associated with neuroblastoma site of origin. **A)** Manhattan plot illustrating common germline variants and their association with neuroblastoma primary site at the *BARD1* gene locus. The cohort consists of European-American neuroblastoma patients, and the analysis reflects a case-case comparison of adrenal (n = 707) vs thoracic (n = 320) patients. Each point represents a germline Single nucleotide polymorphism (SNP) or indel polymorphism that was either imputed to 1000 Genomes Project data or directly genotyped by Illumina SNP array. **B)** Manhattan plot of the *BARD1* locus. Each variant's genomic coordinate is plotted on the *x*-axis, and the negative log10 transform of the association *P* value is plotted on the *y*-axis. The color of each point reflects the statistical correlation (r^2) between the top associated rs6720708 (alleles = T/C, adrenal-associated allele = T; odds ratio = 1.74, 95% confidence interval = 1.44 to 2.12, SNPTEST $P = 1.99 \times 10^{-8}$) and surrounding variants at the *BARD1* locus. Another prominent signal on the 14q locus did not replicate in the independent Omni array cohort.

neuroblastoma) were no longer statistically significant when the analysis was restricted to only *MYCN*-nonamplified cases, which may reflect statistical confounding with *MYCN* amplification and/or reduced statistical power in subset analysis. Interestingly, an enrichment of chromosome 11q deletions—a negative prognostic indicator that inversely correlated with *MYCN* amplification (18,19)—in adrenal cases was observed in the *MYCN*-nonamplified subcohort. This finding provides further evidence that chromosome 11q deletion marks an aggressive molecular subclass of neuroblastoma whose enrichment in adrenal cases may partially account for worse clinical outcomes in the absence of *MYCN* amplification.

We observed statistically significant differences in other recurrent genetic alterations between adrenal and thoracic neuroblastoma independently of *MYCN* status. We evaluated recurrent point mutations that differentiate adrenal and thoracic neuroblastomas, observing a surprising relative paucity of *ALK* mutations among adrenal tumors. Interestingly, this difference in *ALK* mutation prevalence increased when the analysis was restricted to only *MYCN*-nonamplified cases. This suggests *ALK* mutations may play important roles in tumorigenesis of thoracic as compared with adrenal neuroblastoma, independent from *MYCN* status. This hypothesis might appear to be in contrast with prior preclinical models suggesting that *ALK* mutations work *in combination* with *MYCN* amplification in the resulting high-risk phenotypes (20,21), although there is one published preclinical model of an ALK-driven neuroblastoma (22). Importantly, we only included recurrent *ALK* mutations that had been identified as "driver mutations" with transformative ability (23), excluding likely passenger mutations.

In our analysis of TARGET gene expression data, we found that gene expression signatures of adrenal and thoracic neuroblastoma are largely predicted by underlying somatic DNA lesions. The lack of a clear differential expression signature

based on primary site after adjusting for MYCN amplification and chromosome 11q loss suggests that adrenal and thoracic neuroblastomas, rather than representing distinct molecular subclasses of neuroblastoma, are each heterogeneous entities, albeit with vastly different propensities toward molecular subclass-defining lesions. One possibility is that the respective microenvironments of adrenal and thoracic niches exert selective pressure inherently favoring specific genetic lesions, whereas another possibility is that temporal biases in mutation occurrence differentially align with critical windows in sympathetic nervous system development during which adrenal and thoracic neuroblastomas arise.

We also investigated whether common germline variation—previously associated with differential susceptibility to neuroblastoma—may also correlate with neuroblastoma primary site. Our study revealed a strong association signal with adrenal primary compared with thoracic at the previously reported *BARD1* tumor suppressor locus (see Figure 5). Notably, the most highly associated rs6720708 SNP was in strong linkage disequilibrium with the putative rs17489363 functional SNP and replicated in an independent European-American cohort. Among other previously reported loci, only variation within *CASC15* showed slight association with adrenal vs thoracic primary site. We did not observe any statistically significant differential association between adrenal and thoracic neuroblastomas for other SNPs at the *HACE1*, *LIN28B*, or *LMO1* loci. However, the adrenal-favored allele was concordant with the previously reported risk allele at all loci, suggesting that the lack of statistical significance may arise from insufficient statistical power and larger studies are required to resolve whether these variants are associated with primary site. Although *BARD1* variants are associated with *MYCN*-amplified and high-risk disease (24), the association of *BARD1* with adrenal neuroblastoma occurs independently of MYCN amplification status.

We identified several limitations in our study. First, high-risk cases are overrepresented in the TARGET cohort, likely resulting in underrepresentation of thoracic cases. Second, neuroblastoma primary site annotation was missing or ambiguous in 373 cases and separate genomic assays were often only available on nonoverlapping TARGET subsets, limiting our ability to perform joint statistical analysis and assess primary site as an independent predictor of survival. Lastly, our current analyses only focus on the genomic profile of tumor cells and did not account for the possible role of the tumor microenvironment. Recent evidence suggests important roles for tumor microenvironment in disease progression (25), which may contribute to the clinical differences between thoracic and adrenal neuroblastoma.

In conclusion, our results collectively support our hypothesis that there are differences in genetic profiles that account for inferior outcomes in adrenal compared with thoracic cases. Our findings have several important clinical and biological implications. With 16% of thoracic tumors harboring *ALK* mutations, routine sequencing for these mutations in this setting should be considered. Additionally, foundational investigation focused on the developmental pathway and segmental chromosomal aberrations that underlie differences in localization may provide novel insights into the fundamental pathogenesis of neuroblastoma. Recent work in the zebrafish model has shown clear differences in sites of origin for malignant neuroblastic transformation (20,26). Thus, although there are many functional consequences reported for the genetic aberrations considered here that help to explain the prognostic differences in primary sites, it is our hope that future validation experiments in developmental animal models of neuroblastoma may shed light on differences in localization.

Funding

This work was supported in part by National Institutes of Health grants T32-HG000046 (DAO), F30-CA192831-01A1 (DAO), P01-CA 217959 (JMM, KKM), R35-CA 220500 (JMM), the Alexandra Scott Lemonade Foundation (KKM), the Strouss Endowed Chair (KKM), and the Giulio D'Angio Endowed Chair (JMM).

Notes

Affiliations of authors: Department of Pediatrics, Children's Hospital of Philadelphia and Perelman School of Medicine at the University of Pennsylvania, Philadelphia, PA (DAO, DR, ZV, YPM, SJD, JMM); Department of Pathology and Laboratory Medicine, Hospital of the University of Pennsylvania, Philadelphia, PA (DAO); Department of Pediatrics, UCSF Benioff Children's Hospital and UCSF School of Medicine, San Francisco, CA (BT, KKM); Dana-Farber/Boston Children's Cancer and Blood Disorders Center and Harvard Medical School, Boston, MA (SGD).

The funders had no role in the design of the study; the collection, analysis, and interpretation of the data; the writing of the manuscript; and the decision to submit the manuscript for publication.

The authors have no conflicts of interest to disclose.

Presented in part at the 49th Congress of the International Society of Paediatric Oncology (SIOP 2017).

References

1. Goodman NW. An open letter to the Director General of the Cancer Research Campaign. *J R Coll Physicians Lond*. 1999;33(1):93.
2. Smith MA, Seibel NL, Altekruse SF, et al. Outcomes for children and adolescents with cancer: challenges for the twenty-first century. *J Clin Oncol*. 2010; 28(15):2625–2634.
3. Matthay KK, Maris JM, Schleiermacher G, et al. *Nat Rev Dis Primers*. 2016 Nov 10;2:16078. doi: 10.1038/nrdp.2016.78. Review. PMID: 27830764
4. Vo KT, Matthay KK, Neuhaus J, et al. Clinical, biologic, and prognostic differences on the basis of primary tumor site in neuroblastoma: a report from the international neuroblastoma risk group project. *J Clin Oncol*. 2014;32(28): 3169–3176.
5. Brodeur GM, Pritchard J, Berthold F, et al. Revisions of the international criteria for neuroblastoma diagnosis, staging, and response to treatment. *J Clin Oncol*. 1993;11(8):1466–1477.
6. Park JR, Bagatell R, London WB, et al. Children's Oncology Group's 2013 blueprint for research: neuroblastoma. *Pediatr Blood Cancer*. 2013;60(6):985–993.
7. Schleiermacher G, Mosseri V, London WB, et al. Segmental chromosomal alterations have prognostic impact in neuroblastoma: a report from the INRG project. *Br J Cancer*. 2012;107(8):1418–1422.
8. Thompson D, Vo KT, London WB, et al. Identification of patient subgroups with markedly disparate rates of MYCN amplification in neuroblastoma: a report from the International Neuroblastoma Risk Group project. *Cancer*. 2016; 122(6):935–945.
9. Campbell K, Gastier-Foster JM, Mann M, et al. Association of MYCN copy number with clinical features, tumor biology, and outcomes in neuroblastoma: a report from the Children's Oncology Group. *Cancer*. 2017;123(21): 4224–4235.
10. Mosse YP, et al. Identification of ALK as a major familial neuroblastoma predisposition gene. *Nature*. 2008;455(7215):930–935.
11. Janoueix-Lerosey I, Lequin D, Brugières L, et al. Somatic and germline activating mutations of the ALK kinase receptor in neuroblastoma. *Nature*. 2008; 455(7215):967–970.
12. Chen Y, Takita J, Choi YL, et al. Oncogenic mutations of ALK kinase in neuroblastoma. *Nature*. 2008;455(7215):971–974.
13. George RE, Sanda T, Hanna M, et al. Activating mutations in ALK provide a therapeutic target in neuroblastoma. *Nature*. 2008;455(7215):975–978.
14. Capasso M, Devoto M, Hou C, et al. Common variations in BARD1 influence susceptibility to high-risk neuroblastoma. *Nat Genet*. 2009;41(6):718–723.

ARTICLE

15. Cimmino F, Avitabile M, Diskin SJ, et al. Fine mapping of 2q35 high-risk neuroblastoma locus reveals independent functional risk variants and suggests full-length BARD1 as tumor-suppressor. *Int J Cancer*. 2018;143(11):2828–2837.
16. Huang M, Weiss WA. Neuroblastoma and MYCN. *Cold Spring Harb Perspect Med*. 2013;3(10):A014415.
17. Niemas-Teshiba R, Matsuno R, Wang LL, et al. MYC-family protein overexpression and prominent nucleolar formation represent prognostic indicators and potential therapeutic targets for aggressive high-MKI neuroblastomas: a report from the children's oncology group. *Oncotarget*. 2018;9(5):6416–6432.
18. Attiyeh EF, London WB, Mossé YP, et al. Chromosome 1p and 11q deletions and outcome in neuroblastoma. *N Engl J Med*. 2005;353(21):2243–2253.
19. Mlakar V, Jurkovic Mlakar S, Lopez G, et al. 11q deletion in neuroblastoma: a review of biological and clinical implications. *Mol Cancer*. 2017;16(1):114.
20. Zhu S, Lee J-S, Guo F, et al. Activated ALK collaborates with MYCN in neuroblastoma pathogenesis. *Cancer Cell*. 2012;21(3):362–373.
21. Montavon G, et al. Wild-type ALK and activating ALK-R1275Q and ALK-F1174L mutations upregulate Myc and initiate tumor formation in murine neural crest progenitor cells. *Oncotarget*. 2014;5(12):4452–4466.
22. Heukamp LC, Thor T, Schramm A, et al. Targeted expression of mutated ALK induces neuroblastoma in transgenic mice. *Sci Transl Med*. 2012;4(141):141ra91.
23. Bresler SC, Weiser DA, Huwe PJ, et al. ALK mutations confer differential oncogenic activation and sensitivity to ALK inhibition therapy in neuroblastoma. *Cancer Cell*. 2014;26(5):682–694.
24. Hungate EA, et al. Evaluation of genetic predisposition for MYCN-amplified neuroblastoma. *J Natl Cancer Inst*. 2017;109(10):1–4.
25. Borriello L, Seeger RC, Asgharzadeh S, et al. More than the genes, the tumor microenvironment in neuroblastoma. *Cancer Lett*. 2016;380(1):304–314.
26. Zhu S, Zhang X, Weichert-Leahey N, et al. LMO1 synergizes with MYCN to promote neuroblastoma initiation and metastasis. *Cancer Cell*. 2017;32(3):310–323.e5.